Approximate Convolution with Pairs of Cubic Bézier LN Curves

Young Joon Ahn [a] and Christoph M. Hoffmann [b]

[a] *Department of Mathematics Education, Chosun University, Gwangju, 501–759, South Korea*

[b] *Department of Computer Science, Purdue University, West Lafayette, IN 47907, USA*

Abstract

In this paper we present an approximation method for the convolution of two planar curves using a pair of two cubic Bézier curves with linear normals (LN). We characterize the necessary and sufficient conditions for two compatible cubic Bézier LN curves to have the same linear normal map. Using this characterization, we obtain the cubic spline approximation of the convolution curve. As illustration, we apply our method to the approximation of a font where the letters are constructed as the Minkowski sum of two planar curves. We also present numerical results using our approximation method for offset curve and compare our method to previous results.

1 Introduction

We revisit the problem of computing the convolution of two curves, a problem with a long history that has delivered many interesting and elegant insights[5,12,15,19,18,21,22]. Closely related is problem of computing Minkowski sums and the special case of computing offsets. These problems have a local and a global aspect. The local aspect involves finding points on the convolved curve or on the offset curve, whereas the global aspect involves trimming parts of the curve not on the outer boundary. Our approach employs cubic Bézier curves with linear normals (LN) to approximate general curves. We coordinate the approximation of the two curves to be convolved so that the local convolution operation becomes trivial. Our study includes error bounds and

Email addresses: ahn@chosun.ac.kr (Young Joon Ahn), cmh@cs.purdue.edu (Christoph M. Hoffmann).

derivations of conditions of nonsingularity of the approximants. A number of examples illustrates our method.

There have been numerous studies on convolution, Minkowski sums, and offset computations[2–4,6,7,9,13,14,16,17,23,24], and we do not review them all. Piegl and Tiller [20] develop algorithms to offset NURBS curves and surfaces accounting for special cases such as circles. They use a curvature-guided sampling approach and interpolate the resulting set of offset points. Ahn et al.[1] approaches offsetting Bézier curves by approximating the circle with Bézier curves of degree equal to the degree of the curve to be offset and gives error bounds.

Lee et al.[15] study Minkowski sums of planar curves. Both the local and global problem dimensions are explored. This paper introduces the notion of compatible curve subdivisions, using segments for which the normals lie in the same interval of directions. Sampoli [21] considers the Minkowski sum of surfaces with linear normals (LN), proving that the Minkowski sum of two LN patches of degree n is a rational surface of degree $2n$. The paper proposes to approximate general surfaces with a macro patch of LN surfaces consisting of four triangular patches. In [22], Sampoli et al. extends the work by considering the convolution of a rational LN surface with a rational Bézier surface. They show that the resulting surface is rational. In [19], Peternell and Steiner consider the Minkowski sum of 3D objects bounded by surfaces permitting a quadratic approximation. At that level of generality, they prove basic properties of Minkowski sum but rely on sampling to solve the global problem.

Peternell and Odehnal [18] prove that quadratic Bézier surfaces are LN and show how to reparameterize them making this property explicit. They consider this problem in the context of convolution.

In this paper, we restrict to the curve case. Our approach is to approximate the curves to be convolved by cubic LN curves to within a prescribed tolerance, and then to compute the convolution. Let B be the base curve, C the curve with which to convolve it. Our approximation is characterized by using pairs of curves, one element approximating a part of B, the other approximating a part of C, such that both approximants have the same normal map. This makes the convolution of the two trivial.

As an application, we present a font approximation using our method. The font is constructed by the Minkowski sum of two planar curves. Our method can yields, within a prescribed tolerance, a cubic spline approximation of the boundary of the Minkowski sum, which is the convolution of two curves. We can find easily the local and global singularities of the cubic spline, and so obtain the trimmed cubic spline approximation for the boundary of the font.

Naturally, our method can be applied to approximate the offset of a planar curve. We present the results of our approximation method for the example studied by Lee et al.[14]

We present our material as follows: In Section 2 we review preliminaries and sketch how to avoid singularities. In Section 3, we derive a simple characterization of cubic Bézier LN curves and explain when those curves have a singularity in the interval [0,1]. We also sketch how global singualrities can be found. In Section 4 we derive conditions for two cubic LN curves to have the same normal map. Such pairs simplify the convolution operation. In Section 5 we illustrate our method for a font approximation. The boundaries of the font are convolutions of two planar curves for which we obtain the cubic spline approximation. In Section 6 we apply our method to approximate the offset of planar curves, and compare our results to other previous ones for the same example.

2 Definitions and Preliminaries

We consider cubic Bézier curves whose control points are constructed from three points $\mathbf{b}_0$, $\mathbf{b}_m$, and $\mathbf{b}_3$ by choosing two parameters δ_0 and δ_1, in $(0, 1)$ and defining the points

$$\mathbf{b}_1 = (1 - \delta_0)\mathbf{b}_0 + \delta_0\mathbf{b}_m$$
$$\mathbf{b}_2 = (1 - \delta_1)\mathbf{b}_3 + \delta_1\mathbf{b}_m$$

The cubic Bézier curve will have the control points $\mathbf{b}_0, \mathbf{b}_1, \mathbf{b}_2, \mathbf{b}_3$. The construction is shown in Figure 1.

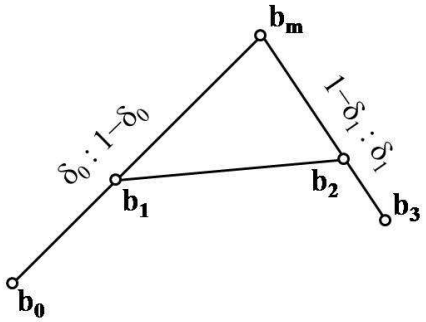

Fig. 1. Control point construction

By imposing specific constraints on the choice of δ_0 and δ_1, we will show that the curves are LN and are not singular in the interior. In particular, we will set

$$\tau \notin [0,1]$$
$$\delta_0 = \frac{2\tau}{3\tau - 1}$$
$$\delta_1 = \frac{2(\tau - 1)}{3\tau - 2}$$

and prove that the resulting cubic Bézier curves are LN and nonsingular in $[0,1]$. When $\tau = \infty$, the cubic curve becomes quadratic.

Let $\nabla \mathbf{b}_0 = \mathbf{b}_m - \mathbf{b}_0$ and $\nabla \mathbf{b}_1 = \mathbf{b}_3 - \mathbf{b}_m$. We define λ as the length ratio of those two vectors, and define

$$\kappa = \frac{3\tau - 1}{3\tau - 2} \cdot \lambda$$

With these quantities we then express the normal map explicitly and derive conditions for two cubic Bézier LN curves to have the same normal map.

Consider the curve arc C_k where S_k is the unit normal at the left end of the arc and E_k the unit normal at the right end of the arc. Two arcs C_1 and C_2 are *compatible* if $S_1 = S_2$ and $E_1 = E_2$. We are interested in finding compatible LN curves that have the same normal map.

When convolving nonsingular curves, the resulting curve may have cuspidal singularities and self-intersections. We call the former a *local singularity* and the latter a *global singularity*. Note that an individual LN curve segment cannot have a global singularity. We will give conditions for the nonsingularity of individual cubic LN curves in the next section. Later, we will show how to avoid singularities in the convolution of two nonsingular, compatible LN curves.

Because of the LN property, an individual curve segment cannot have a self-intersection. Thus global singularities arise when two approximants of the convolution intersect. There are several ways to discover such singularities. We can enclose each curve segment within a convex polygon, using the convex hull property. Such polygons can then be intersected to narrow the search of candidates for intersection, so lowering the asymptotic complexity in the number of approximants n. For example, using enclosing rectangles, we can lower the intersection complexity from $O(n^2)$ to $O(n \log^2(n) + J)$, where J is the number of intersecting pairs; e.g., [10], Chapter 3.

A different approach would be to exploit the capabilities of graphics coprocessors (GPUs). Briefly, the approximant is rendered into the frame buffer, a highly parallel operation that can be accomplished in the fraction of a second in most cases, whereupon the intersections are read out by a pixel mask scan. The details are routine. The potential issue with this approach is the fixed

resolution of the rendering phase. It can be overcome by rendering at a scale commensurate with the prescribed tolerance and, if necessary, re-rendering critical areas at higher resolution, so "zooming in" to potential intersections. See also [11].

3 Cubic LN Bézier Curves

We derive conditions for when a cubic Bézier curve is LN. Moreover, we give conditions under which cubic LN Bézier curves do not have a cuspidal singularity. Note that since we assume that the curve is LN there cannot be a self-crossing singularity since it would require the curve normal to turn more than π.

Our construction of a cubic LN curve in Bézier form rests on a geometric property involving the first and last curve point and the intersection of the tangents to the curve at those end points.

Let three points $\mathbf{b}_0$, $\mathbf{b}_m$ and $\mathbf{b}_3$ be given. We will find a cubic Bézier LN curve $\mathbf{b}(t) = (x(t), y(t))$ with the control points

$$[\mathbf{b}_0,\ ((1-\delta_0)\mathbf{b}_0 + \delta_0\mathbf{b}_m),\ ((1-\delta_1)\mathbf{b}_3 + \delta_1\mathbf{b}_m,\ \mathbf{b}_3]$$

for a suitable choice of δ_0 and δ_1. Thus, the curve is

$$\mathbf{b}(t) = B_0^3(t)\mathbf{b}_0 + B_1^3(t)((1-\delta_0)\mathbf{b}_0 + \delta_0\mathbf{b}_m) + B_2^3(t)((1-\delta_1)\mathbf{b}_3 + \delta_1\mathbf{b}_m) + B_3^3(t)\mathbf{b}_3$$

where t is in $[0, 1]$ and the $B_i^n(t)$ are the Bernstein polynomials of degree n.

The derivative of $\mathbf{b}(t)$ is $(x'(t), y'(t))$ where each component polynomial is of degree 2. Assume that the curve has a cusp; that is, assume that $x'(t)$ and $y'(t)$ vanish simultaneously at $t = \tau$:

$$x'(\tau) = y'(\tau) = 0$$

This condition is equivalent to

$$\delta_0 = \frac{2\tau}{3\tau - 1} \qquad \text{and} \qquad \delta_1 = \frac{2(\tau - 1)}{3\tau - 2} \tag{1}$$

See also Figure 2. Evidently $\mathbf{b}(t)$ does not have a cusp in $[0, 1]$ iff $\tau \notin [0, 1]$. So, we should choose

$$\tau \in (-\infty, 0) \cup (1, \infty]$$

Note that for $\tau = \infty$ or $-\infty$ we obtain $\delta_0 = \delta_1 = 2/3$ which means that the cubic LN curve is a quadratic Bézier curve in that case.

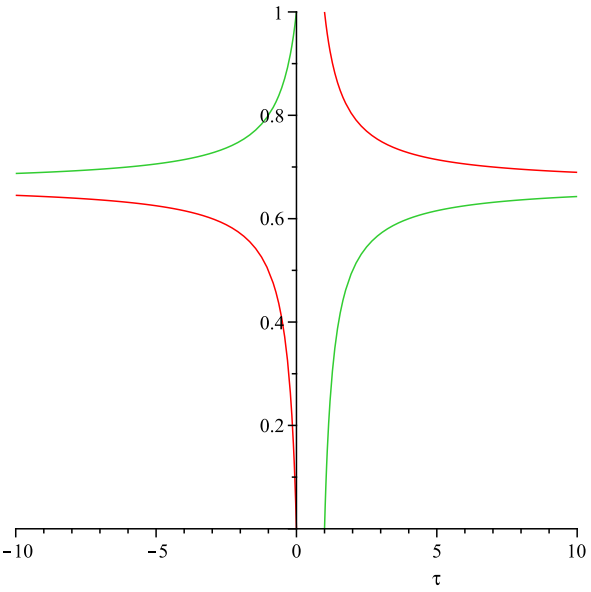

Fig. 2. The cubic LN curve is determined from δ_0 (red) and δ_1 (green) after choosing τ. The curve will be regular in $[0,1]$ iff $\tau \in (-\infty, 0) \cup (1, \infty]$.

For τ in that range, δ_0 and δ_1 are both contained in $[0,1]$, so that the cubic LN curve does not have any cusp, loop or inflection point is regular in $[0,1]$.

We prove next that this construction results in LN curves. By simple calculation,

$$\mathbf{b}'(t) = -\frac{6(t-\tau)\{(3\tau-2)(\mathbf{b}_m - \mathbf{b}_0)(1-t) + (3\tau-1)(\mathbf{b}_3 - \mathbf{b}_m)t\}}{(3\tau-1)(3\tau-2)}$$

Let $\nabla\mathbf{b}_0 = \mathbf{b}_m - \mathbf{b}_0$ and $\nabla\mathbf{b}_1 = \mathbf{b}_3 - \mathbf{b}_m$. The tangent vector of $\mathbf{b}(t)$ is parallel to

$$(3\tau-2)\nabla\mathbf{b}_0(1-t) + (3\tau-1)\nabla\mathbf{b}_1 t$$

or equivalently, the normal vector of $\mathbf{b}(t)$ is parallel to

$$(3\tau-2)\mathbf{n}_0(1-t) + (3\tau-1)\mathbf{n}_1 t \tag{2}$$

where $\mathbf{n}_i = R\nabla\mathbf{b}_i$ and $R = \begin{pmatrix} 0 & -1 \\ 1 & 0 \end{pmatrix}$ is a rotation by $\pi/2$. Clearly, the normal vector is also parallel to

$$(3\tau-2)\cdot N_0 \cdot (1-t) + (3\tau-1)\cdot\lambda\cdot N_1 \cdot t \tag{3}$$

where $\lambda = \frac{|\nabla\mathbf{b}_1|}{|\nabla\mathbf{b}_0|}$ and N_i is the unit normal in the direction of $\mathbf{n}_i$.

Summarizing, we have

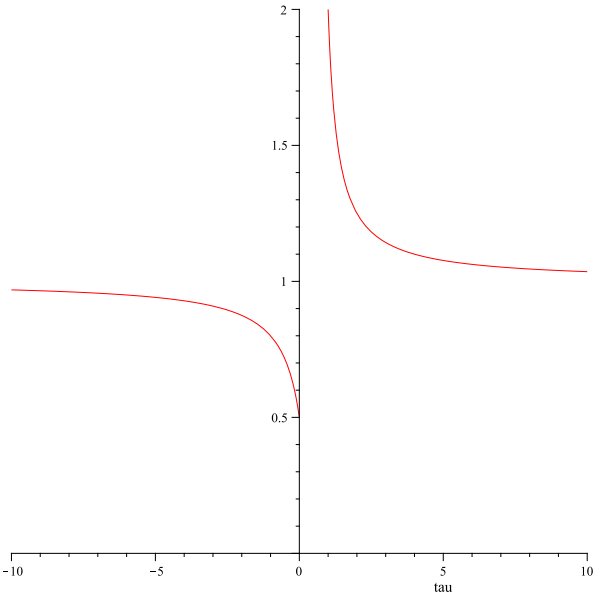

Fig. 3. $\tau \to \frac{3\tau-1}{3\tau-2}$, for $\tau \in (-\infty, 0) \cup (1, \infty]$. The range is $(\frac{1}{2}, 2)$.

PROPOSITION 3.1 *Given three points* $\mathbf{b}_0, \mathbf{b}_m, \mathbf{b}_3$ *that are not collinear and a number* $\tau \in (-\infty, 0) \cup (1, \infty]$*, the cubic Bezier curve with control points*

$$[\mathbf{b}_0,\ ((1-\delta_0)\mathbf{b}_0 + \delta_0\mathbf{b}_m),\ ((1-\delta_1)\mathbf{b}_3 + \delta_1\mathbf{b}_m,\ \mathbf{b}_3]$$

is a regular LN curve in $[0, 1]$*, where* δ_0 *and* δ_1 *are given by (1).*

4 Pairs of LN Curves With Polynomial Convolution

In this section we derive conditions under which a pair of cubic LN Bézier curves has the same linear normal vector map. Such curves can be convolved by adding the two function values. The linear normal vectors of such a pair of cubic LN Bézier curves we search are

$$N_0 \cdot (1-t) + \kappa \cdot N_1 \cdot t$$

for all $t \in [0, 1]$.

By Equation (3), the regular cubic LN curve satisfies

$$\mathbf{b}'(t) \perp N_0 \cdot (1-t) + \frac{3\tau-1}{3\tau-2} \cdot \lambda \cdot N_1 \cdot t \tag{4}$$

for some $\tau \in (-\infty, 0) \cup (1, \infty]$. Using this fact we get the following lemma.

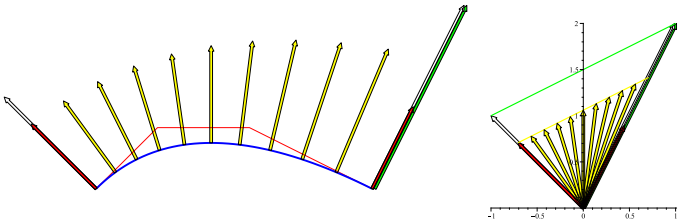

(a) $\kappa = \lambda$, $\tau = \infty$, $[\delta_0, \delta_1] = [2/3, 2/3]$

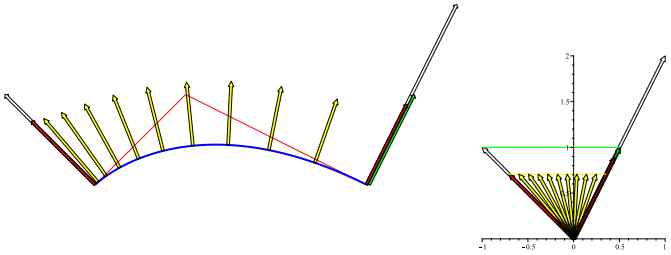

(b) $\kappa = \lambda/2$, $\tau = 0$, $[\delta_0, \delta_1] = [0, 1]$

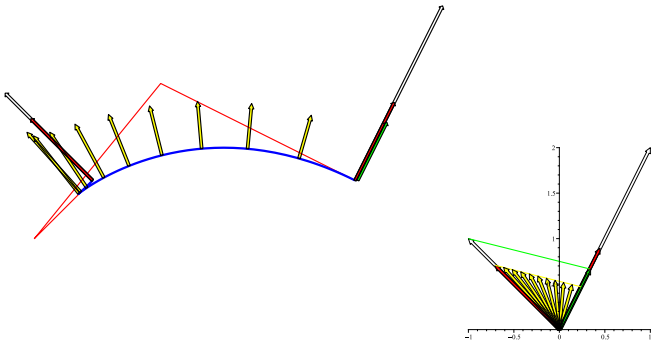

(c) $\kappa = \lambda/3$, $\tau = 1/6$, $[\delta_0, \delta_1] = [-\frac{2}{3}, \frac{10}{9}]$

Fig. 4. The blue cubic LN curve depends on the value κ and has the linear normal vector $N_0 \cdot (1-t) + \kappa \cdot N_1 \cdot t$, shown by the yellow arrows. The control polygon of cubic LN Bézier curve is drawn in red. The red vectors are the unit normal vectors N_i, and the white vectors are the normal vectors $\mathbf{n}_i$, $i = 0, 1$. The green vector is κ/λ times of $\mathbf{n}_1$ (right white arrow). The green line is passing through the end points of $\mathbf{n}_0$ and $(\kappa/\lambda)\mathbf{n}_1$, and represents the linear normal map of the cubic LN curve.
(a) the blue cubic LN curve is regular and is the quadratic Bézier case.
(b) the blue cubic LN curve has a singularity at $t = 0$, but it has no singularity in the interior and has continuous unit tangent vector.
(c) the blue cubic LN curve has a cusp at $t = 1/6$.

LEMMA 4.1 *The cubic LN Bézier curve* $\mathbf{b}(t)$ *is regular if and only if*

$$\mathbf{b}'(t) \perp N_0 \cdot (1-t) + \kappa \cdot N_1 \cdot t$$

for some $\kappa \in (\lambda/2, 2\lambda)$.

Proof. Let $\mathbf{b}(t)$ be regular. Then $\tau \in (-\infty, 0) \cup (1, \infty]$ and

$$\frac{3\tau - 1}{3\tau - 2} = 1 + \frac{1}{3\tau - 2} \in (\frac{1}{2}, 2),$$

as shown in Figure 3. Putting

$$\kappa = \frac{3\tau - 1}{3\tau - 2} \cdot \lambda,$$

by Equation (4) we have $\mathbf{b}'(t) \perp N_0 \cdot (1-t) + \kappa \cdot N_1 \cdot t$ and $\kappa \in (\lambda/2, 2\lambda)$.

Conversely, let $\mathbf{b}'(t) \perp N_0 \cdot (1-t) + \kappa \cdot N_1 \cdot t$ for some $\kappa \in (\lambda/2, 2\lambda)$. Then Equation (4) yields $\kappa = \frac{3\tau-1}{3\tau-2} \cdot \lambda$ or equivalently

$$\tau = \begin{cases} \frac{2\kappa - \lambda}{3(\kappa - \lambda)}, & (\kappa \neq \lambda) \\ \infty, & (\kappa = \lambda) \end{cases},$$

and Equation (1) yields

$$\delta_0 = \frac{2}{3}\left(2 - \frac{\lambda}{\kappa}\right) \text{ and } \delta_1 = \frac{2}{3}\left(2 - \frac{\kappa}{\lambda}\right). \tag{5}$$

Since $\kappa \in (\lambda/2, 2\lambda)$, we obtain $\delta_0, \delta_1 \in (0, 1)$ and hence the cubic LN Bézier curve $\mathbf{b}(t)$ is regular. □

Consider two cubic LN Bézier curves $\mathbf{b}_l(t)$ and $\mathbf{b}_r(t)$ having the polygons $[\mathbf{b}_0^l, \mathbf{b}_m^l, \mathbf{b}_3^l]$ and $[\mathbf{b}_0^r, \mathbf{b}_m^r, \mathbf{b}_3^r]$, and let $\lambda_l = |\nabla \mathbf{b}_1^l|/|\nabla \mathbf{b}_0^l|$ and $\lambda_r = |\nabla \mathbf{b}_1^r|/|\nabla \mathbf{b}_0^r|$. Two planar regular curves $\mathbf{b}_l$ and $\mathbf{b}_r$ are called *compatible* if their *Gauss maps* are equal, i.e., $\mathbf{N}(\mathbf{b}_l) = \mathbf{N}(\mathbf{b}_r)$, where $\mathbf{N}(\mathbf{b})$ is unit normal vector field of $\mathbf{b}$. For more knowledge of compatible pair or Gauss map, refer to [15]. Now, we present the sufficient and necessary condition for a pair of compatible cubic LN Bézier curves $\mathbf{b}_l(t)$ and $\mathbf{b}_r(t)$ to have the same linear normal vector map.

PROPOSITION 4.2 *Two compatible cubic LN curves* $\mathbf{b}_l(t)$ *and* $\mathbf{b}_r(t)$ *have the same linear normal vector map, i.e.,* $\mathbf{b}_l'(t) \parallel \mathbf{b}_r'(t)$ *for all* $t \in [0, 1]$ *if and only if*

$$\frac{1}{4} < \frac{\lambda_r}{\lambda_l} < 4. \tag{6}$$

Furthermore, if $\mathbf{b}_l'(t) \parallel \mathbf{b}_r'(t)$*, then the convolution curve* $\mathbf{b}_l * \mathbf{b}_r$ *can be obtained by*

$$(\mathbf{b}_l * \mathbf{b}_r)(t) = \mathbf{b}_l(t) + \mathbf{b}_r(t).$$

Proof. Let $\mathbf{b}_l'(t) \parallel \mathbf{b}_r'(t)$ for all $t \in [0,1]$. By Lemma 3.1,

$$\mathbf{b}_l'(t) \perp N_0 \cdot (1-t) + \kappa_l \cdot N_1 \cdot t$$

for some $\kappa_l \in (\lambda_l/2, 2\lambda_l)$ and

$$\mathbf{b}_r'(t) \perp N_0 \cdot (1-t) + \kappa_r \cdot N_1 \cdot t$$

for some $\kappa_r \in (\lambda_r/2, 2\lambda_r)$. Since $\mathbf{b}_l'(t) \parallel \mathbf{b}_r'(t)$ for all $t \in [0,1]$, we have $\kappa_l = \kappa_r$. Thus $(\lambda_l/2, 2\lambda_l) \cap (\lambda_r/2, 2\lambda_r)$ should not be empty, which is equivalent to $\frac{1}{4} < \frac{\lambda_r}{\lambda_l} < 4$.

Conversely, let $\frac{1}{4} < \frac{\lambda_r}{\lambda_l} < 4$. Then $(\lambda_l/2, 2\lambda_l) \cap (\lambda_r/2, 2\lambda_r)$ is not empty. We can take κ in the nonempty set. By Lemma 3.1,

$$\mathbf{b}_l'(t) \perp N_0 \cdot (1-t) + \kappa \cdot N_1 \cdot t \quad \text{and} \quad \mathbf{b}_r'(t) \perp N_0 \cdot (1-t) + \kappa \cdot N_1 \cdot t$$

for the same κ. Thus we have $\mathbf{b}_l'(t) \parallel \mathbf{b}_r'(t)$ for all $t \in [0,1]$. □

REMARK 4.3 *For $\tau = 0$, the cubic LN Bézier curve $\mathbf{b}(t)$ has a singular point at $t = 0$. Even if the unit tangent vector $T(t)$ does not exist at $t = 0$, we can define the unit tangent vector at $t = 0$ using the one-sided limit $T(0)^+ = \lim_{t\to 0+} T(t)$ which gives $\mathbf{b}(t)$ the continuous unit tangent vector, as shown in Figure 4(b). By same construction, we obtain the (extended) linear normal vector for all $t \in [0,1]$. Therefore, we can expand Proposition 4.2 slightly as follows. Two compatible cubic LN curves $\mathbf{b}_l(t)$ and $\mathbf{b}_r(t)$ have the same (extended) linear normal vector map, if and only if*

$$\frac{1}{4} \le \frac{\lambda_r}{\lambda_l} \le 4. \tag{7}$$

We illustrate our proposition. As shown in Figure 5(a), the start points $\mathbf{b}_0^l$ and $\mathbf{b}_0^r$, end points $\mathbf{b}_3^l$ and $\mathbf{b}_3^r$, and the unit normal vectors N_0 and N_1 (red colored vectors) are given as follows:

$$\mathbf{b}_0^l = [2.5, -1], \mathbf{b}_0^r = [2.5, -4], N_0 = \langle -\frac{4}{5}, \frac{3}{5} \rangle$$
$$\mathbf{b}_3^l = [3.5, 5],\ \mathbf{b}_3^r = [2, -\frac{7}{6}],\ N_1 = \langle -\frac{1}{\sqrt{2}}, -\frac{1}{\sqrt{2}} \rangle$$

Then we have the mid-points $\mathbf{b}_m^l = [.5, 1]$, $\mathbf{b}_m^r = [1, -2.5]$, and the ratios $\lambda_l = \frac{5\sqrt{2}}{4} \approx 1.77$, $\lambda_r = \frac{5\sqrt{2}}{9} \approx 0.786$. Since λ_l and λ_r satisfy Equation (7), we may choose κ in the interval $[5\sqrt{2}/4.5, 5\sqrt{2}/2] \approx [0.884, 1.57]$. We take κ as

$$\kappa = \sqrt{\lambda_l \cdot \lambda_r} = \frac{5\sqrt{2}}{6} \approx 1.18,$$

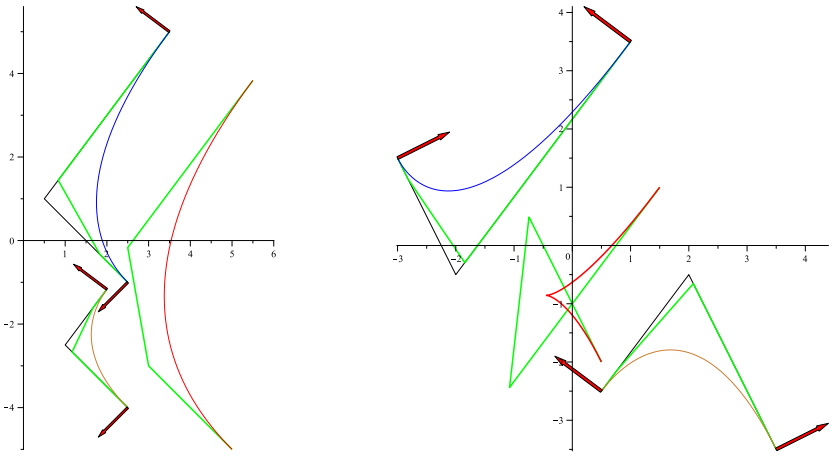

(a) (b)

Fig. 5. Convolutions:
(a) Cubic LN Bézier curves $\mathbf{b}_l(t)$, blue, and $\mathbf{b}_r(s)$, gold, and their convolution curve $\mathbf{b}_l * \mathbf{b}_r$, red.
(b) Cubic LN Bézier curves $\mathbf{b}_l(t)$, blue, and $\mathbf{b}_r(s)$, gold, and their convolution curve $\mathbf{b}_l * \mathbf{b}_r$, red thick-lines, which has a cusp.
The control polygons are plotted by green color. The mid points $\mathbf{b}_m^l$ and $\mathbf{b}_m^r$ are the corner points of black polygons.

the geometric mean of λ_l and λ_r. By Equation (5), we have

$$[\delta_0^l, \delta_1^l] = [\frac{1}{3}, \frac{8}{9}], \qquad [\delta_0^r, \delta_1^r] = [\frac{8}{9}, \frac{1}{3}]$$

fixing the control polygons (drawn green) of the cubic LN Bézier curves. The derivative vectors of the cubic LN Bézier curves $\mathbf{b}_l(t)$ and $\mathbf{b}_r(t)$ are

$$\mathbf{b}_l'(t) = \frac{2(3t+1)}{3}\langle 6t-3, t+3\rangle$$
$$\mathbf{b}_r'(t) = \frac{-3t+4}{3}\langle 6t-3, t+3\rangle$$

and they are parallel for all $t \in [0,1]$, so that the normal vectors $N_l(t)$ and $N_r(t)$ are also parallel at the same $t \in [0,1]$. Hence we can obtain easily the (red) convolution curve

$$(\mathbf{b}_l * \mathbf{b}_r)(t) = \mathbf{b}_l(t) + \mathbf{b}_r(t)$$

and its (green) control polygon.

The convolution curve of two regular cubic LN Bézier curves may have a cusp as shown in Figure 5(b). Here, the start points and the unit normal vectors (red colored vectors) are given as follows:

$$\mathbf{b}_0^l = [-3, \frac{3}{2}], \mathbf{b}_0^r = [\frac{7}{2}, \frac{-7}{2}], N_0 = \langle \frac{2}{\sqrt{5}}, \frac{1}{\sqrt{5}} \rangle$$
$$\mathbf{b}_3^l = [1, \frac{7}{2}], \mathbf{b}_3^r = [\frac{1}{2}, \frac{-5}{2}], N_1 = \langle -\frac{4}{5}, \frac{3}{5} \rangle$$

We have $\mathbf{b}_m^l = [-2, -1/2]$, $\mathbf{b}_m^r = [2, -1/2]$ and $\lambda_l = \sqrt{5} \approx 2.24$, $\lambda_r = \frac{\sqrt{5}}{3} \approx 0.745$, which satisfy Equation (7), and we choose κ in the interval $[\sqrt{5}/2, 2\sqrt{5}/3]$. We take $\kappa = \sqrt{\lambda_l \cdot \lambda_r} = \sqrt{5/3} \approx 1.29$, and then we have

$$[\delta_0^l, \delta_1^l] = [\frac{4 - 2\sqrt{2}}{3}, \frac{12 - 2\sqrt{3}}{9}] \approx [.179, .948], \qquad [\delta_0^r, \delta_1^r] \approx [.948, .179].$$

The derivative vectors are

$$\mathbf{b}_l'(t) = \frac{6t - 1 + \sqrt{3}}{3} \langle 3(2 - \sqrt{3})(2t + 1 + \sqrt{3}), 2(3 + \sqrt{3})(t + 3 - 2\sqrt{3}) \rangle$$
$$\mathbf{b}_r'(t) = \frac{6t - 5 - \sqrt{3}}{2\sqrt{3}} \langle 3(2 - \sqrt{3})(2t + 1 + \sqrt{3}), 2(3 + \sqrt{3})(t + 3 - 2\sqrt{3}) \rangle$$

They are parallel for all $t \in [0, 1]$. Thus we obtain the (red) convolution curve $(\mathbf{b}_l * \mathbf{b}_r)(t) = \mathbf{b}_l(t) + \mathbf{b}_r(t)$, and its derivative

$$(\mathbf{b}_l * \mathbf{b}_r)'(t) = \frac{6t - 1 - \sqrt{3}}{6} \langle 3(2t + 1 + \sqrt{3}), 2(9 + 5\sqrt{3})(t + 3 - 2\sqrt{3}) \rangle.$$

Thus the convolution curve $\mathbf{b}_l * \mathbf{b}_r$ has a singular point at $\tau = (1 + \sqrt{3})/6 \in (0, 1)$ and we can see that this convolution curve has a cusp, as shown in Figure 5(b). By Equation (1) or by simple calculation of the control points $\mathbf{b}_i = \mathbf{b}_i^l + \mathbf{b}_i^r$, $i = 0, \cdots, 3$ and $\mathbf{b}_m = \mathbf{b}_m^l + \mathbf{b}_m^r$, we also have

$$[\delta_0, \delta_1] = [\frac{4 + 2\sqrt{3}}{3}, \frac{12 + 2\sqrt{3}}{9}] \approx [2.49, 1.72].$$

Using $[\delta_0, \delta_1]$, we can present the necessary and sufficient condition for the convolution curve $\mathbf{b}_l * \mathbf{b}_r$ having cusp as the following proposition.

PROPOSITION 4.4 *The convolution curve* $(\mathbf{b}_l * \mathbf{b}_r)(t) = \mathbf{b}_l(t) + \mathbf{b}_r(t)$ *is also cubic LN curve, and it has a cusp in* $(0, 1)$ *if and only if one of* δ_0 *and* δ_1 *is not in the open interval* $(0, 1)$.

Proof. Since $\mathbf{b}_l(t)$ and $\mathbf{b}_r(t)$ have the same linear normal vector, the convolution curve $(\mathbf{b}_l * \mathbf{b}_r)(t) = \mathbf{b}_l(t) + \mathbf{b}_r(t)$ also has the same linear normal vector. It has a cusp in (0,1) if and only if it has a cusp at $\tau \in (0, 1)$. By Equation (1), $\tau \in (0, 1)$ is equivalent to $\delta_0 \notin (0, 1)$ and to $\delta_1 \notin (0, 1)$. Thus the cubic LN curve $\mathbf{b}_l * \mathbf{b}_r$ has a cusp in $(0, 1)$ if and only if one of δ_0 and δ_1 is not in the open interval $(0, 1)$. □

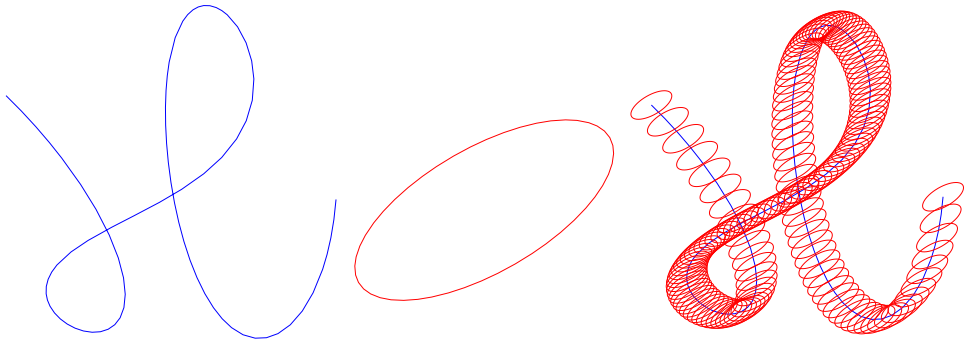

(a) (b) (c)

Fig. 6. (a) The skeleton curve constructed by Bézier curve of degree nine. (b) The cross-section of pen shaped ellipse (c) Minkowski sum

	$TOL = 1$
$t \in [t_{i-1}, t_i]$	$d_H^{\mathbf{P}} + d_H^{\mathbf{Q}}$
$[0, .0985]$	6.91×10^{-2}
$[.0985, .151]$	1.08×10^{-1}
$[.151, t_A]$	7.15×10^{-1}
$[t_A, .526]$	9.95×10^{-2}
$[.526, .632]$	5.42×10^{-2}
$[.632, .710]$	1.22×10^{-1}
$[.710, .877]$	2.66×10^{-1}
$[.877, .935]$	2.30×10^{-2}
$[.935, 1]$	2.89×10^{-2}

	$TOL = 10^{-1}$
$t \in [t_{i-1}, t_i]$	$d_H^{\mathbf{P}} + d_H^{\mathbf{Q}}$
$[0, .0985]$	6.91×10^{-2}
$[.0985, .122]$	3.80×10^{-3}
$[.122, .151]$	3.23×10^{-3}
$[.151, .225]$	4.13×10^{-2}
$[.225, t_A]$	7.71×10^{-2}
$[t_A, .526]$	9.95×10^{-2}
$[.526, .632]$	5.42×10^{-2}
$[.632, .663]$	4.65×10^{-3}
$[.663, .710]$	6.81×10^{-3}
$[.710, .800]$	6.63×10^{-3}
$[.800, .877]$	7.36×10^{-3}
$[.877, .935]$	2.30×10^{-2}
$[.935, 1]$	2.89×10^{-2}

	$TOL = 10^{-2}$
$t \in [t_{i-1}, t_i]$	$d_H^{\mathbf{P}} + d_H^{\mathbf{Q}}$
$[0, .0435]$	6.29×10^{-3}
$[.0435, .0985]$	9.82×10^{-3}
$[.0985, .122]$	3.80×10^{-3}
$[.122, .151]$	3.23×10^{-3}
$[.151, .187]$	2.07×10^{-3}
$[.187, .225]$	1.47×10^{-3}
$[.225, .276]$	1.99×10^{-3}
$[.276, .306]$	3.87×10^{-4}
$[.306, t_A]$	3.06×10^{-3}
$[t_A, .399]$	3.85×10^{-3}
$[.399, .438]$	4.37×10^{-4}
$[.438, .526]$	2.25×10^{-3}
$[.526, .583]$	3.29×10^{-3}
$[.583, .632]$	9.34×10^{-4}
$[.632, .663]$	4.65×10^{-3}
$[.663, .710]$	6.81×10^{-3}
$[.710, .800]$	6.63×10^{-3}
$[.800, .877]$	7.36×10^{-3}
$[.877, .916]$	3.55×10^{-3}
$[.916, .935]$	1.52×10^{-3}
$[.935, .952]$	1.35×10^{-3}
$[.952, 1]$	6.56×10^{-3}

Table 1
The left columns of each tables is t's range of the ninth-degree Bézier curve $\mathbf{p}(t)$. $\mathbf{p}$ has an unique inflection point at $\mathbf{p}(t_A)$ of $t_A = .349$.

The proposition provides a simple check for local singularities when convolving with our method.

5 Application I. Approximation of Convolution Curves

We approximate the convolution curve using our method by pairs of LN cubic Bézier curves.

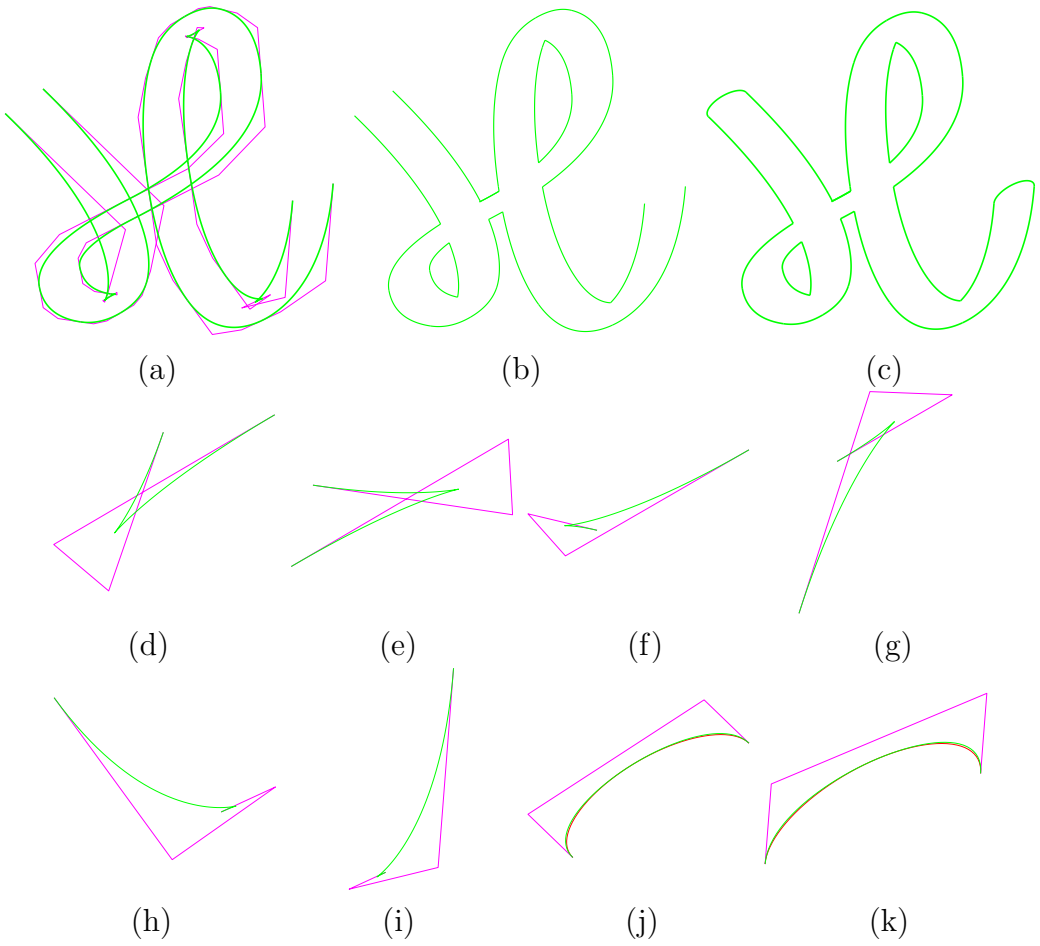

Fig. 7. (a) The convolution curves (green) of cubic LN curves $\mathbf{p}^a * \mathbf{q}^a$ and their control polygons (magenta). The result comprises 26 cubic Bézier curves achieving a tolerance within $TOL = 10^{-1}$. It has six cusps.
(b) The construction of a font character using the trimmed convolution approximation.
(c) The font 'H' with two segments of the cubic Bézier curve to close both ends of the font.
(d)-(i) The cubic LN approximants (green) that have a cusp, and their control polygons (magenta).
(j)-(k) The cubic Bézier approximation (green) of half ellipse (red), and their control polygons (magenta).

Let two planar curves be given. One is a Bézier curve of degree nine, $\mathbf{p}(t)$ with $t \in [0, 1]$, whose control points are $(.2, 6.6)$, $(8.9, -1.8)$, $(7.2, -15.8)$, $(-43.4, 41.8)$, $(70.8, -41.3)$, $(-29.6, 30.4)$, $(20.9, 20.0)$, $(-6.1, 4.1)$, $(8.2, -7.8)$, and $(9.1, 3.8)$, as shown in Figure 6(a). The other is an ellipse $\mathbf{q}(s)$ whose major and minor axes are 1.4 and 0.6, rotated by an angle of $\pi/6$, as shown in Figure 6(b). Let the ellipse move along the Bézier curve. Their Minkowki sum defines a font character 'H' as shown in Figure 6(c). The Bézier curve $\mathbf{p}(t)$ is the skeleton

curve and the ellipse $\mathbf{q}(s)$ is the cross section of pen. We use the pair of cubic LN Bézier curves $\mathbf{p}^a$ and $\mathbf{q}^a$ to approximate the convolution curve $\mathbf{p} * \mathbf{q}$.

In constructing the approximation, we use a divide and conquer method. The curve should be subdivided first at singular points and inflection points, since an approximating cubic LN Bézier curve should not have those points. The ninth-degree Bézier curve $\mathbf{p}(t)$ has an unique inflection point at $t = t_A \approx 0.349$, at which the curve should be subdivided first.

If the subdivided segment $\mathbf{p}(t)$, $t \in [a, b]$ is C^1-continuous and has neither singularity nor inflection point, then $\arg(\mathbf{p}'(t))$ is monotone increasing or decreasing, where $\arg(\cdot)$ is the angle (or argument) of the vector $\mathbf{p}'(t)$ considered as a complex number. Also, if the Gauss map of the segment $\mathbf{p}(t)$, $t \in [a, b]$ is of length greater than π, then the segment is subdivided at the points $t = t_i$, $i = 1, \cdots, k-1$, where k is the smallest integer satisfying

$$\frac{\arg(\mathbf{p}'(b)) - \arg(\mathbf{p}'(a))}{k} < \pi$$

and t_i is the point satisfying

$$\arg(\mathbf{p}'(t_i)) = \arg(\mathbf{p}'(a)) + \frac{i}{k}(\arg(\mathbf{p}'(b)) - \arg(\mathbf{p}'(a))).$$

For this reason, $\mathbf{p}(t)$ is subdivided at $t = .151, .632$ and $.877$.

Now, we find the segment $\mathbf{q}(s)$, $s \in [s_{i-1}, s_i]$ which is compatible with $\mathbf{p}(t)$, $t \in [t_{i-1}, t_i]$, and approximate them simultaneously by a pair of cubic LN curves $\mathbf{p}^a$ and $\mathbf{q}^a$ having the same linear normal map. If two curve segments $\mathbf{p}(t)$, $t \in [t_{i-1}, t_i]$ and $\mathbf{q}(s)$, $s \in [s_{i-1}, s_i]$ do not satisfy Equation (7), then by Remark 3.3, there is no pair of (extended) regular cubic LN curves $\mathbf{p}^a$ and $\mathbf{q}^a$ with the same normal map. Then they should be also subdivided. We can see the asymtotic behavior of the ratios λ_l or λ_r of curve segments $\mathbf{p}$ and $\mathbf{q}$ as follows.

REMARK 5.1 *The ratio λ of any planar polynomial curve, Bézier or spline, converges to 1 quadratically as its length goes to zero, i.e.,*

$$\lambda - 1 = \mathcal{O}(s^2),$$

where s is the arc-length parameter.

We present the proof in the Appendix.

In whole process of this approximation, any two curve segments $\mathbf{p}(t)$, $t \in [t_{i-1}, t_i]$ and $\mathbf{q}(s)$, $s \in [s_{i-1}, s_i]$ always satisfy Equation (7), and so there is at least one pair of (extended) regular cubic LN curves $\mathbf{p}^a$ and $\mathbf{q}^a$. As the error

measurement we use the sum of two Hausdorff distances

$$d_H(\mathbf{p}, \mathbf{p}^a) + d_H(\mathbf{q}, \mathbf{q}^a),$$

instead of $d_H(\mathbf{p} * \mathbf{q}, \mathbf{p}^a * \mathbf{q}^a)$. It is easier to calculate than $d_H(\mathbf{p} * \mathbf{q}, \mathbf{p}^a * \mathbf{q}^a)$ directly.

If the error is larger than the prescribed tolerance, the curve segments $\mathbf{p}(t)$, $t \in [t_{i-1}, t_i]$ and $\mathbf{q}(s)$, $s \in [s_{i-1}, s_i]$ should be subdivided. We have considered the subdivision points as one of the following points:

(a) at t_j and s_j such that
$\arg(\mathbf{p}'(t_j)) = \arg(\mathbf{q}'(s_j)) = (\arg(\mathbf{p}'(t_{i-1})) + \arg(\mathbf{p}'(t_i)))/2$,
(b) at t_j and s_j such that
$\arg(\mathbf{p}'(t_j)) = \arg(\mathbf{q}'(s_j)) = \arg(\mathbf{p}(t_i) - \mathbf{p}(t_{i-1}) + \mathbf{q}(s_i) - \mathbf{q}(s_{i-1}))$, or
(c) at t_j and s_j such that

$$\begin{aligned}\arg(\mathbf{p}'(t_j)) &= \arg(\mathbf{q}'(s_j)) \\ &= \frac{d_H(\mathbf{p}, \mathbf{p}^a) \cdot \arg(\mathbf{p}'(t_M)) + d_H(\mathbf{q}, \mathbf{q}^a) \cdot \arg(\mathbf{q}'(s_M)}{d_H(\mathbf{p}, \mathbf{p}^a) + d_H(\mathbf{q}, \mathbf{q}^a)},\end{aligned}$$

where t_M and s_M is the point at which the Hausdorff distances $d_H(\mathbf{p}, \mathbf{p}^a)$ and $d_H(\mathbf{q}, \mathbf{q}^a))$ occur.

For our font example we have used subdivision method (c). The subdivisions of the curves are needed until the error is less than the prescribed tolerance.

As shown in Table 1, the number of subdivisions needed to achieve the tolerances $TOL = 1, 0.1$ and 0.01 are 6, 12 and 21, respectively. Figure 7(a) shows the the approximate cubic Bézier spline $\mathbf{p}^a * \mathbf{q}^a$ of the convolution curve $\mathbf{p} * \mathbf{q}$ for $TOL = 10^{-1}$. The approximation has six cusps, and we plot the Bézier curves having the cusps and their control polygons in Figures 7(d)-(i).

The intersection points of cubic Bézier curves can be found easily, we can obtain the trimmed cubic spline, as shown in Figure 7(b). At both end of the font, there are two half ellipses. We approximate them by cubic Bézier curves using Floater's spline approximation method of conic section[8]. The cubic approximant is G^1 interpolation of ellipse at both end points and at the middle point of the ellipse, as shown in Figures 7(j)-(k), and their approximation errors are 8.81×10^{-3} and 1.03×10^{-2}, in order. Finally, we obtain the font after the whole process of approximations, as shown in Figure 7(c).

6 Application II. Approximation of Offset Curves

In this section we apply our method to the approximation of offset curves. We will use convolution with a circle and proceed as in Application I.

Let $\mathbf{p}$ be a planar curve and r be the offset distance. We approximate $\mathbf{p}$ and $\mathbf{c}_r$ by two compatible cubic Bézier curves $\mathbf{p}^a$ and $\mathbf{c}_r^a$, where $\mathbf{c}_r$ is the circular arc of radius r and centered at origin, and is compatible with $\mathbf{p}^a$. As an error measurement, we use

$$d_H(\mathbf{p}, \mathbf{p}^a) + r \cdot d_H(\mathbf{c}, \mathbf{c}^a) \tag{8}$$

instead of $d_H(\mathbf{p} * \mathbf{c}_r, \mathbf{p}^a * \mathbf{c}_r^a)$, where $\mathbf{c}$ is the unit circular arc compatible to $\mathbf{c}_r$, and $\mathbf{c}^a$ is its cubic LN approximation of $\mathbf{c}$ by our method. The Hausdorff distance $d_H(\mathbf{c}, \mathbf{c}^a)$ can be obtained directly as follows:

PROPOSITION 6.1 *Let $\mathbf{c}$ be the unit circular arc with angle $2\alpha < \pi$, and $\mathbf{c}^a$ be its cubic LN Bézier approximation having the linear normal map*

$$\mathbf{n}(t) = N_0 \cdot (1-t) + \kappa \cdot N_1 \cdot t$$

The Hausdorff distance between circular arc $\mathbf{c}(t)$ and its cubic LN approximation $\mathbf{c}^a(s)$ is

$$d_H(\mathbf{c}, \mathbf{c}^a) = \begin{cases} |\|\mathbf{c}^a(s_1)\| - 1|, & (\kappa \in [\frac{1}{2}, 1-\sin\alpha] \cup [\frac{1}{1-\sin\alpha}, 2]) \\ \max\{|\|\mathbf{c}^a(s_1)\| - 1|, |\|\mathbf{c}^a(s_2)\| - 1|\} & \\ & (\kappa \in (1-\sin\alpha, \frac{1}{1+\sin\alpha}) \cup (1+\sin\alpha, \frac{1}{1-\sin\alpha})) \\ |\|\mathbf{c}^a(s_2)\| - 1|, & (\kappa \in [\frac{1}{1+\sin\alpha}, 1+\sin\alpha]) \end{cases}$$

where

$$s_1 = \frac{-B + \sqrt{B^2 - 4AC}}{2A}, \qquad s_2 = \frac{-B - \sqrt{B^2 - 4AC}}{2A}. \tag{9}$$

and

$$\begin{aligned} A &= (\kappa-1)^3 + 4\kappa(\kappa-1)\sin^2\alpha \\ B &= 2(\kappa-1)^2 + \kappa(-5\kappa+3)\sin^2\alpha \\ C &= -(\kappa-1)^2 + \kappa^2\sin^2\alpha. \end{aligned} \tag{10}$$

We give the proof of the proposition in the appendix.

As an example, we approximate the r-offset of the cubic Bézier curve using Equation (8) and Proposition 6.1, as shown in Figure 8(a), which was presented by Lee et. al. in [14]. The data in Table 2 is from Lee et. al. [14] and

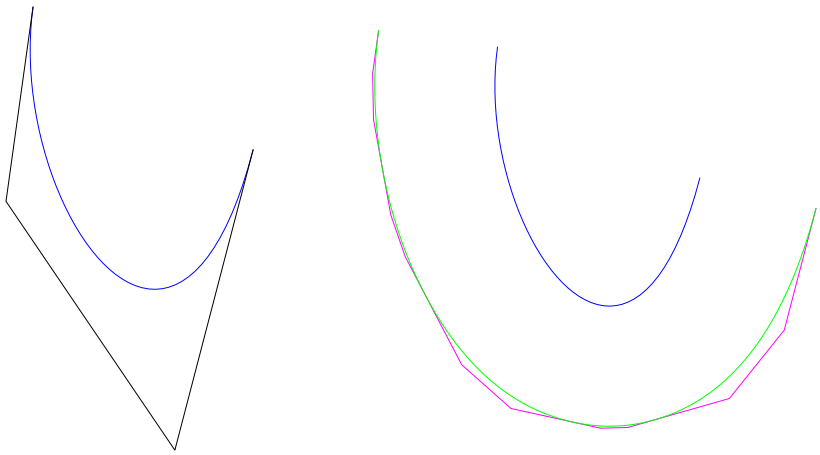

(a) (b)

Fig. 8. (a) The cubic Bézier curve (blue) and its control polygon (black).
(b) For the tolerance $TOL = 10^{-2}$, our approximation curve $\mathbf{p}^a * \mathbf{c}_r^a$ is the green cubic spline, and its control polygon (magenta) has 16 control points.

TOL	Cob	Elb	Elb2	Til	Lst	Lst2	M_2	Piegl/Til	our method
10^{-1}	10	11	13	10	7	10	22	6	10
10^{-2}	31	24	25	31	13	19	29	9	16
10^{-3}	94	74	97	97	19	31	43	15	28
10^{-4}	316	216	247	322	31	46	71	25	43
10^{-5}	865	974	769	886	50	88	127	43	79

Table 2
Our method adapts the divide and conquer method, and uses $d_H(\mathbf{p}, \mathbf{p}^a)+r\cdot d_H(\mathbf{c}, \mathbf{c}^a)$ for the error measurement. The column of M_2 is from the method of Lee et. al. [14]

Piegl and Tiller [20]. We added our approximation results in the last column of the table. For the tolerance $TOL = 10^{-2}$, our method required four subdivisions and, using the pair of cubic LN Bézier curves $\mathbf{p}^a$ and $\mathbf{c}_r^a$, yielded a cubic spline with 16 control points, as shown in Figure 8(b).

Acknowledgements: This work was supported in part by National Research Foundation of Korea Grant funded by the Korean Government(KRF-2008-313-C00120). Additional support is by NSF Grants CPATH CCF-0722210 and CCF-0938999, DOE award DE-FG52-06NA26290, and by a gift from Intel Corporation.

References

[1] Y. J. Ahn, Y. S. Kim, and Y. Shin. Approximation of circular arcs and offset curves by Bézier curves of high degree. *J. Comp. Appl. Math.*, 167:405–416, 2004.

[2] M. Aigner, B. Jütler, L. Gonzalez-Vega, and J. Schicho. Parameterizing surfaces with certain special support functions, including offsets of quadrics and rationally supported surfaces. *J. Symb. Comp.*, 44:180–191, 2009.

[3] B. Bastl, B. Jüttler, J. Kosinka, and M. Lávička. Computing exact rational offsets of quadratic triangular bezier surface patches. *Comp. Aided Desi.*, 40:197–209, 2008.

[4] G. Elber, I. K. Lee, and M. S. Kim. Comparing offset curve approximation method. *IEEE Comp. Grap. Appl.*, 17(3):62–71, 1997.

[5] R. T. Farouki and J. Hass. Evaluating the boundary and covering degree of planar minkowski sums and other geometrical convolutions. *J. Comp. Appl. Math.*, 209:246–266, 2007.

[6] R. T. Farouki, B. Jütler, and C. Manni. Pythagorean-hodograph curves and related topics. *Comp. Aided Geom. Desi.*, 25:203–204, 2008.

[7] R. T. Farouki and T. W. Sederberg. Analysis of the offset to a parabola. *Comp. Aided Geom. Desi.*, 12(6):639–645, 1995.

[8] M. Floater. An $O(h^{2n})$ Hermite approximation for conic sectoins. *Comp. Aided Geom. Desi.*, 14:135–151, 1997.

[9] J. Gravesen, B. Jütler, and Z. Šír. On rationally supported surfaces. *Comp. Aided Geom. Desi.*, 25:320–331, 2008.

[10] C. Hoffmann. *Geometric and Solid Modeling: An Introduction.* Morgan Kaufman, San Mateo, CA, 1989. on the web.

[11] C. Hoffmann, C.-S. Chiang, and P. Rosen. Hardware assistance for constrained circle constructions I. *Computer Aided Design and Applications*, page to appear, 2010.

[12] S. Hur and T. Kim. Finding the best conic approximation to the convolution curve of two compatible conics based on Hausdorff distance. *Comp. Aided Desi.*, 41:513–524, 2009.

[13] M. Lávička and B. Bastl. PN surfaces and their convolutions with rational surfaces. *Comp. Aided Geom. Desi.*, 25:763–774, 2008.

[14] I. K. Lee, M. S. Kim, and G. Elber. Planar curve offset based on circle approximation. *Comp. Aided Desi.*, 28:617–630, 1996.

[15] I. K. Lee, M. S. Kim, and G. Elber. Polynomial/rational approximation of Minkowski sum boundary curves. *Graphical Models and Image Processing*, 60:136–165, 1998.

[16] W. Lü. Rational offsets by reparametrizations. *preprint*, 1992.

[17] H. P. Moon. Equivolumetric offset surfaces. *Comp. Aided Geom. Desi.*, 26:17–36, 2009.

[18] M. Peternell and B. Odehnal. Convolution surfaces of quadratic triangular Bézier surfaces. *Comp. Aided Geom. Desi.*, 25:116–129, 2008.

[19] M. Peternell and T. Steiner. Minkowski sum boundary surfaces of 3D objects. *Graph. Models*, 69:180–190, 2007.

[20] L. Piegl and W. Tiller. Computing offsets of NURBS curves and surfaces. *Comp. Aided Desi.*, 31:147–156, 1999.

[21] M. Sampoli. Computing the convolution and the Minkowski sum of surfaces. In *Proc. 21st Spring Conference on Computer Graphics*, pages 111 – 117, 2005.

[22] M. Sampoli, M. Peternell, and B. Jüttler. Exact parameterization of convolution surfaces and rational surfaces with linear normals. *Comp. Aided Geom. Desi.*, 23:179–192, 2006.

[23] J. Sanchez-Reyes. Offset-rational sinusoidal spirals in bezier form. *Comp. Aided Geom. Desi.*, 24(3):142–150, 2007.

[24] F. San Segundo and J. R. Sendra. Partial degree formulae for plane offset curves. *J. Symb. Comp.*, 44:635–654, 2009.

Appendix

We now prove Remark 5.1 and Proposition 6.1. The following proves Remark 5.1.

Proof. Let $\mathbf{b}(t)$ be a planar polynomial curve, and $\mathbf{b}^*(s) = \mathbf{b}(t(s))$ be the reparametrization of the arc-length parameter s. Then $\mathbf{b}^*(s)$ has the Taylor series near $s = 0$ as follows

$$\mathbf{b}^*(s) = \mathbf{b}^*(0)+T\cdot s+\kappa\cdot N\cdot\frac{s^2}{2}+\cdots = \mathbf{b}^*(0)+T\cdot(s+\mathcal{O}(s^3))+\kappa\cdot N\cdot(\frac{s^2}{2}+\mathcal{O}(s^3))$$

where T and N are unit tangent and unit normal vectors at $s = 0$, and κ is the curvature at that point. The derivative is

$$\frac{d\mathbf{b}^*(s)}{ds} = T\cdot(1+\mathcal{O}(s^2))+\kappa\cdot N\cdot(s+\mathcal{O}(s^2)).$$

Let consider the curve $\mathbf{b}$ in the interval $[0, s]$. Then the vector form of tangent lines at both end points 0 and s are

$$\mathbf{b}^*(0)+T\cdot t \quad \text{and} \quad \mathbf{b}^*(s)+\{T\cdot(1+\mathcal{O}(s^2))+\kappa\cdot N\cdot(s+\mathcal{O}(s^2))\}t'.$$

The latter tangent line is

$$\mathbf{b}^*(0)+T\cdot\{s+\mathcal{O}(s^3)+(1+\mathcal{O}(s^2))t'\}+\kappa\cdot N\cdot\{\frac{s^2}{2}+\mathcal{O}(s^3)+(s+\mathcal{O}(s^2))t'\}.$$

Thus at $t' = -\frac{s}{2}+\mathcal{O}(s^2)$ and at $t = \frac{s}{2}+\mathcal{O}(s^3)$, they have the intersection point

$$\mathbf{b}_m = \mathbf{b}^*(0)+T\cdot(\frac{s}{2}+\mathcal{O}(s^3))$$

so

$$\nabla\mathbf{b}_0 = \mathbf{b}_m-\mathbf{b}^*(0) = T\cdot(\frac{s}{2}+\mathcal{O}(s^3))$$
$$\nabla\mathbf{b}_1 = \mathbf{b}^*(s)-\mathbf{b}_m = T\cdot(\frac{s}{2}+\mathcal{O}(s^3))+\kappa\cdot N\cdot(\frac{s^2}{2}+\mathcal{O}(s^3))$$

and

$$\|\nabla\mathbf{b}_1\| = \sqrt{(\frac{s}{2}+\mathcal{O}(s^3))^2+\kappa^2(\frac{s^2}{2}+\mathcal{O}(s^3))^2} = \frac{s}{2}+\mathcal{O}(s^3)$$

Thus we have

$$\lambda-1 = \frac{\|\nabla\mathbf{b}_1\|}{\|\nabla\mathbf{b}_0\|}-1 = \frac{\frac{s}{2}+\mathcal{O}(s^3)}{\frac{s}{2}+\mathcal{O}(s^3)}-1 = \mathcal{O}(s^2)$$

□

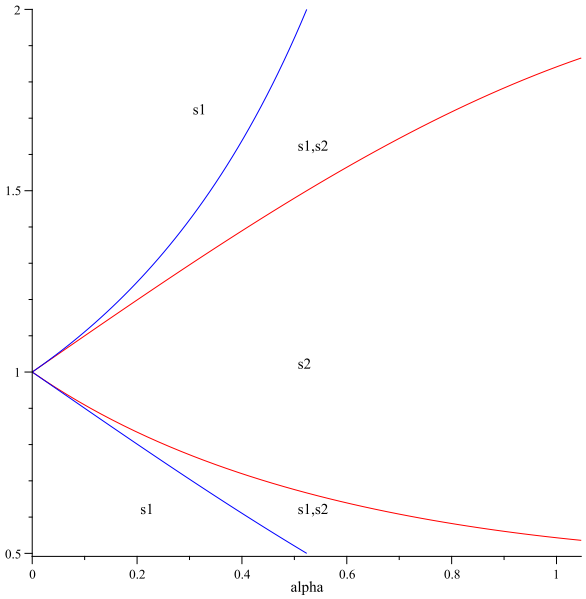

Fig. 9. The range of (α, κ) for s_1 and $s_2 \in (0,1)$, in the α, κ-plane, $(\alpha, \kappa) \in (0, \pi/2) \times [1/2, 2]$.
$s_1 \in (0,1) \Leftrightarrow \kappa \in (\frac{1}{2}, \frac{1}{1+\sin\alpha}) \cup (1+\sin\alpha, 2)$ (bounded by red curves).
$s_2 \in (0,1) \Leftrightarrow \kappa \in (1-\sin\alpha, \frac{1}{1-\sin\alpha})$ (bounded by blue curves).

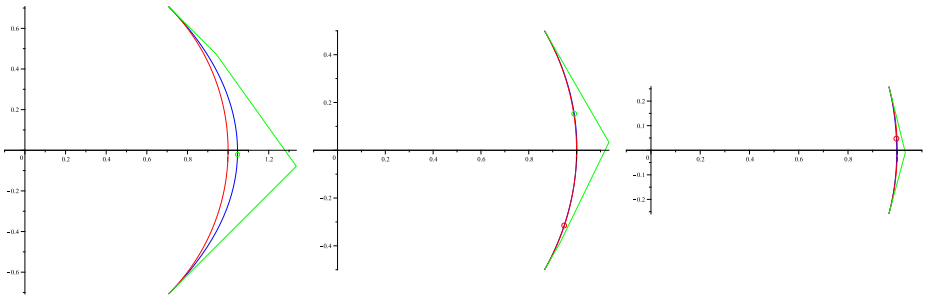

Fig. 10. The circular arc(red curve) and its cubic LN approximation (blue curve) with the control polygon(green). The Hausdorff distance occurs at s_1(small red circle) or s_2 (small green circle). From left to right, $(\alpha, \kappa) = (\frac{\pi}{4}, 1.5), (\frac{\pi}{6}, 0.6)$, and $(\frac{\pi}{12}, 1.8)$, respectively.

Next, we prove Proposition 6.1 as follows.

Proof. With out loss of generality we assume that the circular arc of angle $2\alpha < \pi$ is given by

$$\mathbf{c}(s) = (\cos s, \sin s), \quad s \in [-\alpha, \alpha].$$

For the linear normal vector

$$\mathbf{n}(t) = [\cos\alpha, -\sin\alpha](1-t) + \kappa \cdot [\cos\alpha, \sin\alpha]t$$

the cubic LN approximation curve is

$$\mathbf{c}^a(s) = \sum \mathbf{c}_i B_i^3(t)$$

with the control points

$$\begin{aligned}
&\mathbf{c}_0 = [\cos\alpha, -\sin\alpha], \qquad \mathbf{c}_1 = [\cos\alpha, -\sin\alpha](1-\delta_0) + [\sec\alpha, 0]\delta_0 \\
&\mathbf{c}_2 = [\cos\alpha, \sin\alpha](1-\delta_1) + [\sec\alpha, 0]\delta_1, \qquad \mathbf{c}_3 = [\cos\alpha, \sin\alpha]
\end{aligned}$$

where

$$\delta_0 = \frac{2}{3}\left(2 - \frac{1}{\kappa}\right), \qquad \delta_1 = \frac{2}{3}(2-\kappa) \tag{11}$$

from Equation (5), since the unit circular arc $\mathbf{c}$ has $\lambda = 1$. Let $f(s) = \|\mathbf{c}^a(s)\| - 1$ and $g(s) = \mathbf{c}^{a\prime}(s) \circ \mathbf{c}^a(s)$. $f'(s) = 0 \Leftrightarrow g(s) = 0$. Then we have

$$\begin{aligned}
g(s) &= \mathbf{c}^{a\prime}(s) \circ \mathbf{c}^a(s) = \left(\sum_{i=0}^{2} 3\Delta\mathbf{c}_i B_i^2(t)\right) \circ \left(\sum_{i=0}^{3} \mathbf{c}_i B_i^3(t)\right) \\
&= \frac{3}{5}\left(3 \cdot \tan^2\alpha\delta_0^2 - 2 \cdot 2\sin^2\alpha(1-\delta_1)\right) B_1^5(t) \\
&+ \frac{3}{10}\Big(3 \cdot (2\sin^2\alpha\delta_0(1-\delta_1) + \delta_0\delta_1\tan^2\alpha) \\
&\quad +6 \cdot (-2\sin^2\alpha(1-\delta_0)(1-\delta_1) + \tan^2\alpha\delta_0(\delta_1-\delta_0)) - 2\sin^2\alpha\delta_1\Big) B_2^5(t) \\
&+ \frac{3}{10}\Big(2\sin^2\alpha\delta_0 + 6 \cdot (2\sin^2\alpha(1-\delta_0)(1-\delta_1) + \tan^2\alpha\delta_1(\delta_1-\delta_0)) \\
&\quad +3 \cdot (-2\sin^2\alpha\delta_1(1-\delta_0) - \delta_0\delta_1\tan^2\alpha)\Big) B_3^5(t) \\
&+ \frac{3}{5}\left(2 \cdot 2\sin^2\alpha(1-\delta_0) - 3 \cdot \tan^2\alpha\delta_1^2\right) B_4^5(t),
\end{aligned}$$

where $\Delta\mathbf{c}_i = \mathbf{c}_{i+1} - \mathbf{c}_i$, $i = 0, 1, 2$. By Equation (11), we get

$$\begin{aligned}
g(s) &= \frac{12\tan^2\alpha}{\kappa^2} \cdot s(1-s) \cdot \Big[(2\kappa-1)\left((\kappa-1)^2 - \kappa^2\sin^2\alpha\right) \\
&- \left((7\kappa-5)(\kappa-1)^2 + \kappa(13\kappa^2 - 14\kappa + 3)\sin^2\alpha\right) s \\
&- (\kappa-1)\left((2\kappa-7)(\kappa-1)^2 + \kappa(23\kappa-13)\sin^2\alpha\right) s^2 \\
&+ 3(\kappa-1)^2\left((\kappa-1)^2 + 4k\sin^2\alpha\right) s^3\Big]
\end{aligned}$$

It can be factorized as

$$\frac{12\tan^2\alpha}{\kappa^2} \cdot s(1-s) \cdot (3(\kappa-1)s - 2\kappa + 1) \cdot [As^2 + Bs + C]$$

where the coefficients A, B and C satisfy Equation (10).

Then $f(s) = \sqrt{\mathbf{c}^a(s) \circ \mathbf{c}^a(s)} - 1$ has the local extremum at

$$0, 1, \frac{2\kappa - 1}{3(\kappa - 1)}, s_1, s_2$$

where s_1 and s_2 are in Equation (9). Since the first three critical points $0, 1, \frac{2\kappa-1}{3(\kappa-1)}$ for $\kappa \in [1/2, 2]$ cannot lie in the open interval $(0, 1)$, we can ignore them. Moreover, by a simple calculation,

$$0 < s_1 < 1 \quad \Leftrightarrow \quad \kappa < \frac{1}{1 + \sin\alpha} \quad \text{or} \quad \kappa > 1 + \sin\alpha,$$

and

$$0 < s_2 < 1 \quad \Leftrightarrow \quad 1 - \sin\alpha < \kappa < \frac{1}{1 - \sin\alpha},$$

as shown in Figure 9. Thus the Hausdorff distance between the circular arc $\mathbf{c}$ and its cubic LN approximation $\mathbf{c}^a$ is

$$d_H(\mathbf{c}, \mathbf{c}^a) = \begin{cases} |\, \|\mathbf{c}^a(s_1)\| - 1 \,|, & (\kappa \in [\frac{1}{2}, 1 - \sin\alpha] \cup [\frac{1}{1-\sin\alpha}, 2]) \\ \max\{|\, \|\mathbf{c}^a(s_1)\| - 1 \,|,\ |\, \|\mathbf{c}^a(s_2)\| - 1 \,|\} & \\ & (\kappa \in (1 - \sin\alpha, \frac{1}{1+\sin\alpha}) \cup (1 + \sin\alpha, \frac{1}{1-\sin\alpha})) \\ |\, \|\mathbf{c}^a(s_2)\| - 1 \,|, & (\kappa \in [\frac{1}{1+\sin\alpha}, 1 + \sin\alpha]). \end{cases}$$

□

For $(\kappa, \alpha) = (\pi/4, 1.5)$, only s_2 is inside of the interval (0,1), for $(\kappa, \alpha) = (\pi/6, 0.6)$, both of s_1 and s_2 are in (0,1), and $(\kappa, \alpha) = (\pi/12, 1.8)$, only s_1 is in (0,1), as shown in Figure 10.